

Theoretical study of fusion reactions $^{32}\text{S} + ^{94,96}\text{Zr}$ and $^{40}\text{Ca} + ^{94,96}\text{Zr}$ and quadrupole deformation of ^{94}Zr

WANG Bing¹, ZHAO WeiJuan¹, ZHAO EnGuang^{2,3}, and ZHOU ShanGui^{2,3,4*}¹Department of Physics, Zhengzhou University, Zhengzhou 450001, China;²State Key Laboratory of Theoretical Physics, Institute of Theoretical Physics, Chinese Academy of Sciences, Beijing 100190, China;³Center of Theoretical Nuclear Physics, National Laboratory of Heavy Ion Accelerator, Lanzhou 730000, China⁴Synergetic Innovation Center for Quantum Effects and Application, Hunan Normal University, Changsha, 410081, China

Received XX, 2015; accepted XX, 2015; published online XX, 2015

The dynamic coupling effects on fusion cross sections for reactions $^{32}\text{S} + ^{94,96}\text{Zr}$ and $^{40}\text{Ca} + ^{94,96}\text{Zr}$ are studied with the universal fusion function formalism and an empirical coupled channel (ECC) model. An examination of the reduced fusion functions shows that the total effect of couplings to inelastic excitations and neutron transfer channels on fusion in $^{32}\text{S} + ^{94}\text{Zr}$ ($^{40}\text{Ca} + ^{94}\text{Zr}$) is almost the same as that in $^{32}\text{S} + ^{96}\text{Zr}$ ($^{40}\text{Ca} + ^{96}\text{Zr}$). The enhancements of the fusion cross section at sub-barrier energies due to inelastic channel coupling and neutron transfer channel coupling are evaluated separately by using the ECC model. The results show that effect of couplings to inelastic excitations channels in the reactions with ^{94}Zr as target should be similar as that in the reactions with ^{96}Zr as target. This implies that the quadrupole deformation parameters β_2 of ^{94}Zr and ^{96}Zr should be similar to each other. However, β_2 's predicted from the finite-range droplet model, which are used in the ECC model, are quite different. Experiments on $^{48}\text{Ca} + ^{94}\text{Zr}$ or $^{36}\text{S} + ^{94}\text{Zr}$ are suggested to solve the puzzling issue concerning β_2 for ^{94}Zr .

Empirical coupled channel model, barrier distribution, universal fusion function, neutron transfer**PACS number(s):** 24.10.-i, 25.60.Pj, 25.40.Hs, 25.70.Jj**Citation:** WANG Bing, ZHAO WeiJuan, ZHAO EnGuang, and ZHOU ShanGui, *Sci. China-Phys. Mech. Astron.*, 58, (2015), doi: ??

1 Introduction

Heavy-ion fusion reaction has been an interesting topic for several decades because the heavy-ion fusion not only is of central importance for nucleosynthesis but also can reveal rich interplay between nuclear structure and reaction dynamics [1–7]. The study of fusion reaction mechanism is also of fundamental importance for understanding the synthesis of superheavy elements, properties of weakly bound nuclei, and symmetry energy of the nuclear equation of state [8–17]. Up to now, lots of important information about fusion dynamics at energies near the Coulomb barrier, especially at sub-barrier energies, are obtained through experimental and theoretical studies, such as the fusion hindrance phenomenon at extreme low energies—a steep falloff of the fusion cross sections [18–23], the role of the neutron transfer effect in the fusion [24–27], the breakup effect on the fusion reactions process [28–35], etc..

In the sub-barrier energy region, a large enhancement of fusion cross section for the fusion reaction of $^{58}\text{Ni} + ^{64}\text{Ni}$ as compared with that for $^{58}\text{Ni} + ^{58}\text{Ni}$ and $^{64}\text{Ni} + ^{64}\text{Ni}$ was observed by Beckerman *et al.* [28]. Broglia *et al.* [29, 30] suggested that the coupling to transfer channels with positive Q values is needed to explain the enhancement of fusion data for the Ni + Ni systems. Large enhancements of sub-barrier fusion cross sections have been also observed in many other reaction systems with positive Q -value neutron transfer (PQNT) channels, such as the reaction systems $^{32}\text{S} + ^A\text{Pd}$ ($A = 104\text{--}106, 108, \text{ and } 110$) [36], $^{40}\text{Ca} + ^{44,48}\text{Ca}$ [37], $^{40}\text{Ca} + ^{94,96}\text{Zr}$ [38, 39], and $^{32}\text{S} + ^{94,96}\text{Zr}$ [40, 41]. For some of these systems, the fusion excitation functions have been measured in sufficiently small energy steps, which can be used to extract the underlying barrier distributions to study the contribution from transfer channels. The experimental barrier distributions are much broader than those of the reaction systems with negative Q -value neutron transfer channel. However,

in some other experiments for reaction systems with PQNT channels [42,43], no enhancement was observed in the fusion cross sections at sub-barrier energies.

Theoretically, many efforts have been made to understand the effect of the neutron transfer channels. In Ref. [31], the authors proposed that a neutron flow between the projectile and the target nuclei before fusion could promote neck formation which provides a force strong enough to overcome the Coulomb force. Therefore the fusion is more favored and the sub-barrier fusion cross section is enhanced. In Ref. [44], Zagrebaev proposed a simplified semiclassical model to describe the effect of neutron transfer on fusion. This effect depends on both neutron transfer probabilities and their Q values. The PQNT provides a gain in the kinetic energy. Consequently, the fusion is easier and the sub-barrier fusion cross section is enhanced. Sargsyan *et al.* suggested that the deformations of the interacting nuclei change owing to the PQNT [45–47]. Thus, the influence of the PQNT channels on fusion is accompanied by and depends on the change of nuclear deformations. In the quantum coupled channel (QCC) model [48], the coupling to PQNT channels is treated approximately by using a macroscopic form factor. Within the microscopic dynamics models, such as the quantum molecular dynamic model [49–54] and the time-dependent Hartree-Fock method [55–61], the effects of surface excitations as well as nucleon transfer can be automatically included. Up to now, although many experiments and theoretical efforts have been devoted to study the mechanism of the coupling to PQNT channels, the underlying mechanism is still far from a clear understanding.

In our previous work [62], a systematic study of capture excitation functions for 217 reaction systems has been performed by using an empirical coupled channel (ECC) model. In the ECC model, a barrier distribution is used to take effectively into account the effects of couplings. The effect of the coupling to PQNT channels is simulated by broadening the barrier distribution. Among these 217 reaction systems, there are 86 systems with positive Q values for one neutron pair transfer channel. The calculated capture cross sections of most of these 86 reaction systems are in good agreement with the experimental values, including $^{32}\text{S} + ^{96}\text{Zr}$ and $^{40}\text{Ca} + ^{96}\text{Zr}$. However, the calculated results underestimate the sub-barrier cross sections for $^{32}\text{S} + ^{94}\text{Zr}$ and $^{40}\text{Ca} + ^{94}\text{Zr}$. These results seem to be similar to those obtained from Ref. [41]. In Ref. [41], a large enhancement for the sub-barrier fusion cross sections was deduced in $^{32}\text{S} + ^{94}\text{Zr}$ compared to $^{32}\text{S} + ^{96}\text{Zr}$ based on QCC calculations without the neutron transfer effect considered, although the $Q(xn)$ values, which are listed in Table 1, for $^{32}\text{S} + ^{94}\text{Zr}$ are relatively smaller than those for $^{32}\text{S} + ^{96}\text{Zr}$. The authors suggested that the neutron transfer effect in $^{32}\text{S} + ^{94}\text{Zr}$ are much stronger than that in $^{32}\text{S} + ^{96}\text{Zr}$. In the present work, we will study the dynamic coupling effects in the reactions $^{32}\text{S} + ^{94,96}\text{Zr}$ and $^{40}\text{Ca} + ^{94,96}\text{Zr}$ with the universal fusion function (UFF) formalism and the ECC model. We will first investigate the dynamic coupling effects

on fusion cross sections with the UFF formalism. Then, the effects of couplings to inelastic excitations and neutron transfer channels on fusion are analysed separately with the ECC model.

The present paper is organized as follows. In Sec. 2, the ECC model is briefly reviewed. The method used to eliminate geometrical factors and static effects of the data is introduced in Sec. 3 where the influence on fusion cross section owing to inelastic excitations and transfer couplings will be also investigated. A summary is given in Sec. 4.

Table 1 Q values for one or multineutron transfer channels from ground state to ground state for $^{32}\text{S} + ^{90,94,96}\text{Zr}$, $^{36}\text{S} + ^{94}\text{Zr}$, $^{40}\text{Ca} + ^{90,94,96}\text{Zr}$, and $^{48}\text{Ca} + ^{90,94,96}\text{Zr}$.

Reaction	$Q(1n)$ (MeV)	$Q(2n)$ (MeV)	$Q(3n)$ (MeV)	$Q(4n)$ (MeV)
$^{32}\text{S} + ^{90}\text{Zr}$	−3.33	−1.23	−6.60	−6.16
$^{32}\text{S} + ^{94}\text{Zr}$	0.42	5.10	3.46	6.15
$^{32}\text{S} + ^{96}\text{Zr}$	0.79	5.74	4.51	7.66
$^{36}\text{S} + ^{94}\text{Zr}$	−3.92	−2.61	−6.88	−6.32
$^{40}\text{Ca} + ^{90}\text{Zr}$	−3.61	−1.44	−5.86	−4.18
$^{40}\text{Ca} + ^{94}\text{Zr}$	0.14	4.89	4.19	8.12
$^{40}\text{Ca} + ^{96}\text{Zr}$	0.51	5.53	5.24	9.64
$^{48}\text{Ca} + ^{90}\text{Zr}$	−6.82	−9.78	−17.31	−20.77
$^{48}\text{Ca} + ^{94}\text{Zr}$	−3.07	−3.45	−7.26	−18.53
$^{48}\text{Ca} + ^{96}\text{Zr}$	−2.71	−2.81	−6.21	−6.95

2 Methods

The fusion cross section at a given center-of-mass energy $E_{\text{c.m.}}$ can be written as the sum of the cross section for each partial wave J ,

$$\sigma_{\text{f}}(E_{\text{c.m.}}) = \frac{\pi\hbar^2}{2\mu E_{\text{c.m.}}} \sum_J^{J_{\text{max}}} (2J+1)T(E_{\text{c.m.}}, J), \quad (1)$$

here μ denotes the reduced mass of the reaction system and T denotes the penetration probability. J_{max} is the critical angular momentum: For the partial wave with angular momentum larger than J_{max} , the “pocket” of the interaction potential disappears. The interaction potential around the Coulomb barrier is approximated by an “inverted” parabola.

The couplings between the relative motion of the two nuclei and other degrees of freedom including the coupling to PQNT channels results in an enhancement in the fusion cross sections at sub-barrier energies. In the ECC model [62], a barrier distribution $f(B)$ is introduced to take into account the coupled channel effects in an empirical way. Then, the penetration probability is calculated as

$$T(E_{\text{c.m.}}, J) = \int f(B)T_{\text{HW}}(E_{\text{c.m.}}, J, B)dB. \quad (2)$$

T_{HW} denotes the penetration probability calculated by the well-known Hill-Wheeler formula [63]. Note that for very

deep sub-barrier penetration, the Hill-Wheeler formula is not valid because of the long tail in the Coulomb potential. In Ref. [64], a new barrier penetration formula was proposed for potential barriers containing a long-range Coulomb interaction and this formula is especially appropriate for the barrier penetration with penetration energy much lower than the Coulomb barrier.

The barrier distribution $f(B)$ is taken to be an asymmetric Gaussian function

$$f(B) = \begin{cases} \frac{1}{N} \exp \left[-\left(\frac{B-B_m}{\Delta_1} \right)^2 \right], & B < B_m \\ \frac{1}{N} \exp \left[-\left(\frac{B-B_m}{\Delta_2} \right)^2 \right], & B > B_m \end{cases} \quad (3)$$

$f(B)$ satisfies the normalization condition $\int f(B)dB = 1$. $N = \sqrt{\pi}(\Delta_1 + \Delta_2)/2$ is a normalization coefficient. Δ_1 , Δ_2 , and B_m denote the left width, the right width, and the central value of the barrier distribution, respectively.

Within the ECC model [62], the barrier distribution is related to the couplings to low-lying collective vibrational states and rotational states. The vibrational modes are connected to the change of nuclear shape. Nuclear rotational states are related to static deformations of the interacting nuclei. Furthermore, when the two nuclei come close enough to each other, both nuclei are distorted owing to the attractive nuclear force and the repulsive Coulomb force, thus dynamical deformations develop [12, 44]. Considering the dynamical deformation, a two-dimensional potential energy surface (PES) with respect to relative distance R and quadrupole deformation of the system can be obtained. Based on the PES, empirical formulas were proposed for calculating the parameters of the barrier distribution in Ref. [62]. Note that such empirical formulas are connected with the quadrupole deformation parameters predicted by the finite-range droplet model (FRDM) [65].

The effect of the coupling to the PQNT channel is simulated by broadening the barrier distribution. Only one neutron pair transfer channel is considered in the ECC model. When the Q value for one neutron pair transfer is positive, the widths of the barrier distribution are calculated as $\Delta_i \rightarrow fQ(2n) + \Delta_i$, ($i = 1, 2$), where $Q(2n)$ is the Q value for one neutron pair transfer. f is taken as 0.32 for all reactions with positive Q value for one neutron pair transfer channel [62].

3 Results and Discussions

The fusion excitation function is influenced by two types of features related to the structure of and interaction potential between the projectile and the target. One is of a static nature, such as the heights, curvatures and radii of the barriers, and the static effects associated with the excess protons or neutrons in weakly bound nuclei. The other one is the dynamic effect of couplings to inelastic excitations, the breakup channel, and nucleon transfer channels. In order to study the

dynamic coupling effects on fusion cross sections, it is necessary to eliminate the geometrical factors and static effects of the potential between the two nuclei [66, 67]. In the present work, we will first investigate the dynamic coupling effects on fusion cross sections by eliminating the static effects with the UFF formalism. Then, the effects of couplings to inelastic excitations and neutron transfer channels on fusion are analysed separately with the ECC model. Since ^{32}S and ^{40}Ca are both well bound, the breakup effects is not important.

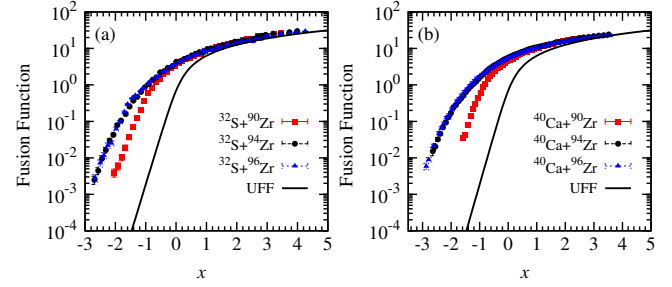


Figure 1 (Color online) The reduced fusion function for reactions (a) $^{32}\text{S} + ^{90,94,96}\text{Zr}$ and (b) $^{40}\text{Ca} + ^{90,94,96}\text{Zr}$ as a function of x . The solid line represents the UFF. The experimental fusion cross sections are taken from Refs. [38–41].

3.1 Reduced fusion excitation functions

We adopt the method proposed in Refs. [66, 67] to eliminate the geometrical factors and static effects of the potential between the two nuclei. According to this prescription, the fusion cross section and the collision energy are reduced to a dimensionless fusion function $F(x)$ and a dimensionless variable x ,

$$F(x) = \frac{2E_{c.m.}}{R_B^2 \hbar \omega} \sigma_F, \quad x = \frac{E_{c.m.} - V_B}{\hbar \omega}, \quad (4)$$

where $E_{c.m.}$ is the collision energy in the center-of-mass frame, σ_F is the fusion cross section, and V_B , $\hbar \omega$, and R_B denote the height, curvature, and radius of the barrier which is approximated by a parabola. The barrier parameters V_B , $\hbar \omega$, and R_B are obtained from the double folding and parameter-free São Paulo potential (SPP) [69–71].

Table 2 The barrier heights, radii, and curvatures used to reduce the fusion excitation functions.

Reaction	V_B (MeV)	$\hbar \omega$ (MeV)	R_B (fm)
$^{32}\text{S} + ^{90}\text{Zr}$	81.37	4.00	10.54
$^{32}\text{S} + ^{94}\text{Zr}$	80.64	3.95	10.64
$^{32}\text{S} + ^{96}\text{Zr}$	80.30	3.90	10.70
$^{40}\text{Ca} + ^{90}\text{Zr}$	99.94	4.02	10.74
$^{40}\text{Ca} + ^{94}\text{Zr}$	99.07	3.97	10.84
$^{40}\text{Ca} + ^{96}\text{Zr}$	98.65	3.97	10.88

If the fusion cross section can be accurately described by the Wong's formula [72]

$$\sigma_F^W(E_{c.m.}) = \frac{R_B^2 \hbar \omega}{2E_{c.m.}} \ln \left[1 + \exp \left(\frac{2\pi(E_{c.m.} - V_B)}{\hbar \omega} \right) \right], \quad (5)$$

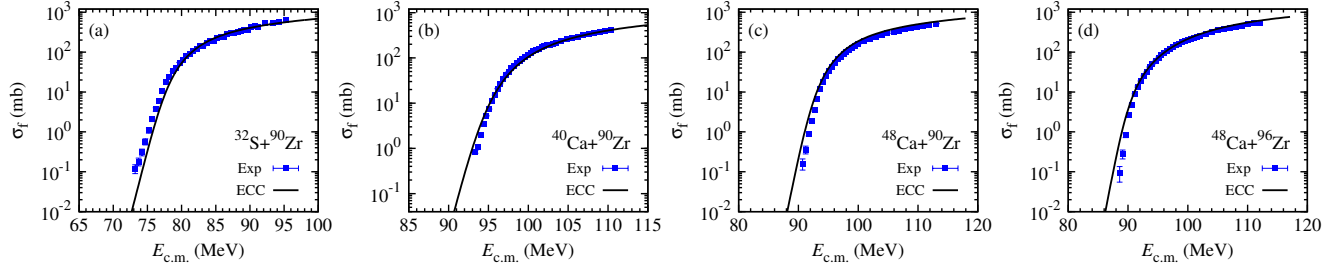


Figure 2 (Color online) The calculated and experimental fusion excitation functions for the reactions (a) $^{32}\text{S} + ^{90}\text{Zr}$, (b) $^{40}\text{Ca} + ^{90}\text{Zr}$, (c) $^{48}\text{Ca} + ^{90}\text{Zr}$, and (d) $^{48}\text{Ca} + ^{96}\text{Zr}$. The solid lines denote the results from the ECC calculations. The experimental fusion excitation functions are taken from Refs. [38, 40, 68].

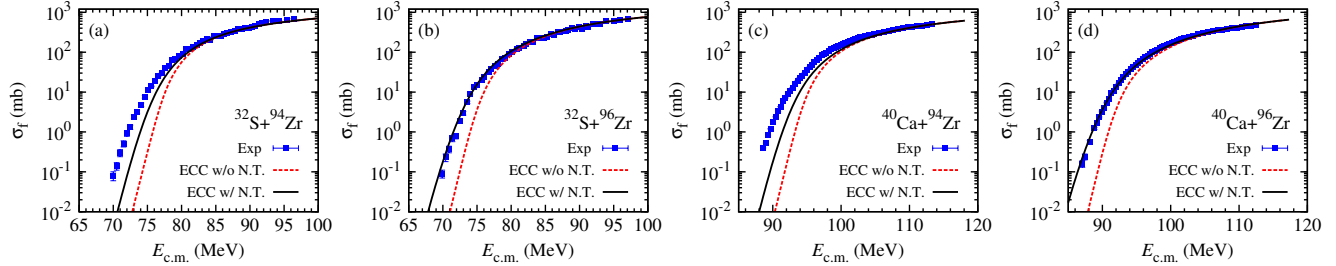


Figure 3 (Color online) The calculated and experimental fusion excitation functions for reactions (a) $^{32}\text{S} + ^{94}\text{Zr}$, (b) $^{32}\text{S} + ^{96}\text{Zr}$, (c) $^{40}\text{Ca} + ^{94}\text{Zr}$, and (d) $^{40}\text{Ca} + ^{96}\text{Zr}$. The dash lines denote the results from the ECC calculations without the coupling to the neutron transfer channels considered. The solid lines denote the results from the ECC calculations with the coupling to the neutron transfer channels considered. The quadrupole deformation parameters of $\beta_2 = 0.062$ and $\beta_2 = 0.217$ are used for ^{94}Zr and ^{96}Zr [65], respectively. The experimental fusion excitation functions are taken from Refs. [38–41].

then $F(x)$ reduces to

$$F_0(x) = \ln[1 + \exp(2\pi x)], \quad (6)$$

which is called the universal fusion function (UFF) [66, 67]. Note that $F_0(x)$ is independent of reaction systems. So $F_0(x)$ is used as a uniform standard reference to explore the coupling effects on fusion cross sections. Deviations of the fusion function from the UFF, if exist, are assumed to mainly arise from the dynamic coupling effects on fusion cross section.

The reduced fusion excitation functions of the reactions $^{32}\text{S} + ^{90,94,96}\text{Zr}$ and $^{40}\text{Ca} + ^{90,94,96}\text{Zr}$ are shown in Fig. 1. The solid lines represent the UFF. The parameters of the potential used in the reduction procedure are obtained from the SPP and listed in Table 2. On one hand, the deviations of the reduced fusion excitation functions from the UFF for $^{32}\text{S} + ^{90,94,96}\text{Zr}$ and $^{40}\text{Ca} + ^{90,94,96}\text{Zr}$ are very large, especially for $^{32}\text{S} + ^{94,96}\text{Zr}$ and $^{40}\text{Ca} + ^{94,96}\text{Zr}$. This implies that the enhancement of the sub-barrier cross sections due to the coupling effects in ^{32}S , $^{40}\text{Ca} + ^{94,96}\text{Zr}$ are much larger than that in ^{32}S , $^{40}\text{Ca} + ^{90}\text{Zr}$. This is because that the neutron transfer channels are opened in ^{32}S , $^{40}\text{Ca} + ^{94,96}\text{Zr}$. The $Q(xn)$ values for the PQNT channels from ground state to ground state for $^{32}\text{S} + ^{90,94,96}\text{Zr}$ and $^{40}\text{Ca} + ^{90,94,96}\text{Zr}$ are shown in Table 1. On the other hand, the behaviors of the reduced fusion excitation functions of $^{32}\text{S} + ^{94}\text{Zr}$ and $^{32}\text{S} + ^{96}\text{Zr}$ are very similar. The situation is the same for the reactions $^{40}\text{Ca} + ^{94,96}\text{Zr}$. This implies that the total effect of the couplings to inelastic excitations and neutron transfer channels in $^{32}\text{S} + ^{94}\text{Zr}$ ($^{40}\text{Ca} +$

^{94}Zr) is almost the same as that in $^{32}\text{S} + ^{96}\text{Zr}$ ($^{40}\text{Ca} + ^{96}\text{Zr}$).

It is well-known that the coupling to PQNT channels enhances the sub-barrier fusion cross section. However, a quantitative understanding of the enhancement due to PQNT channel coupling remains elusive because the only observable is the total enhancement of the cross section. In order to further understand the effect of the neutron transfer channels in these reactions, we will study the effects of couplings to inelastic excitations and neutron transfer channels on fusion separately by using the ECC model.

3.2 Couplings to inelastic excitations and PQNT channels

In this section, we will isolate the effect of transfer coupling from that of couplings to the inelastic excitations channels. We first estimate the enhancement due to inelastic excitations channel couplings alone by adopting the ECC model [62].

The experimental fusion excitation functions and the results from ECC calculations for ^{32}S , $^{40,48}\text{Ca} + ^{90}\text{Zr}$ and $^{48}\text{Ca} + ^{96}\text{Zr}$ are shown in Fig. 2. For these four reactions, the Q values of neutron transfer are negative as seen in Table 1. Therefore, only the couplings to inelastic excitations channels are responsible for the enhancement. The solid lines denote the results from the ECC calculations. In the ECC calculations, the static quadrupole deformation parameters $\beta_2 = 0.035$, $\beta_2 = 0.062$, and $\beta_2 = 0.217$ are used for $^{90,94,96}\text{Zr}$ [65], respectively. One can find that results from the ECC calculations are in good agreement with the data. This implies that the ECC model with the barrier distributions obtained from

Ref. [62] can describe well the effect of the couplings to inelastic excitations channels. Therefore, the ECC calculations can provide an accurate quantitative estimate of the enhancement due to inelastic excitations channel couplings alone.

As mentioned above, the sub-barrier cross section of reactions $^{32}\text{S} + ^{94,96}\text{Zr}$ ($^{40}\text{Ca} + ^{94,96}\text{Zr}$) shows an extra enhancement as compared with that of $^{32}\text{S} + ^{90}\text{Zr}$ ($^{40}\text{Ca} + ^{90}\text{Zr}$). This is because that the PQNT channels are opened in ^{32}S (^{40}Ca) + $^{94,96}\text{Zr}$, c.f. the Q values for neutron transfer listed in Table 1. We first perform the ECC calculations with couplings to the inelastic excitations channels considered only. The comparison of the results from ECC calculations to the experimental values for $^{32}\text{S} + ^{94,96}\text{Zr}$ and $^{40}\text{Ca} + ^{94,96}\text{Zr}$ are shown in Fig. 3 by the dash lines. It can be seen that the experimental fusion data at near-barrier and sub-barrier energy show large enhancement as compared with the ECC calculations without the coupling to neutron transfer channels considered. Consequently, these enhancements may be from the coupling to PQNT channels.

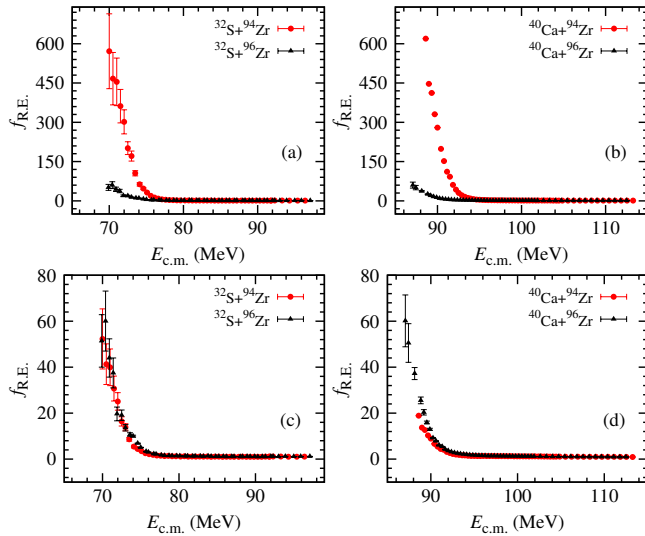


Figure 4 (Color online) The relative enhancement $f_{\text{R.E.}}$ owing to the coupling to PQNT channels for the reactions $^{32}\text{S} + ^{94,96}\text{Zr}$ [(a) and (c)] and $^{40}\text{Ca} + ^{94,96}\text{Zr}$ [(b) and (d)]. The upper panels (a) and (b) show the results obtained with $\beta_2 = 0.062$ for ^{94}Zr used and the lower panels (c) and (d) show the results obtained with $\beta_2 = 0.217$ for ^{94}Zr used. The experimental fusion excitation functions are taken from Refs. [38–41].

In the ECC model, the effect of coupling to the PQNT channels is simulated by broadening the barrier distribution which is related to the $Q(2n)$ value. The results from ECC calculations with the neutron transfer effects taken into account are shown in Fig. 3 by the solid line. For $^{32}\text{S} + ^{96}\text{Zr}$ and $^{40}\text{Ca} + ^{96}\text{Zr}$, it can be seen that the calculated results are in good agreement with the experimental values. But, for $^{32}\text{S} + ^{94}\text{Zr}$ and $^{40}\text{Ca} + ^{94}\text{Zr}$, the calculated results underestimate the sub-barrier cross sections considerably. To understand this underestimation, we follow Jia *et al.* [41] and examine the relative enhancement. The relative enhancement is calculated as the ratio of the experimental fusion cross sec-

tion to the calculated result by using the ECC model without the coupling to the neutron transfer channels considered, i.e., $f_{\text{R.E.}} = \sigma^{\text{exp}}(E_{\text{c.m.}})/\sigma_{\text{ECC}}^{\text{th}}(E_{\text{c.m.}})$. Figure 4 shows these relative enhancements for $^{32}\text{S} + ^{94,96}\text{Zr}$ and $^{40}\text{Ca} + ^{94,96}\text{Zr}$. From Fig. 4(a) and Fig. 4(b), one can find that the relative enhancements for the reactions with ^{94}Zr as target are much larger than those for the reactions with ^{96}Zr as target. This implies that if the estimates of the enhancement due to inelastic excitations channel couplings for the $^{32}\text{S} + ^{94}\text{Zr}$ and $^{40}\text{Ca} + ^{94}\text{Zr}$ are reliable, the effect of PQNT in $^{32}\text{S} + ^{94}\text{Zr}$ ($^{40}\text{Ca} + ^{94}\text{Zr}$) is much stronger than that in $^{32}\text{S} + ^{96}\text{Zr}$ ($^{40}\text{Ca} + ^{96}\text{Zr}$).

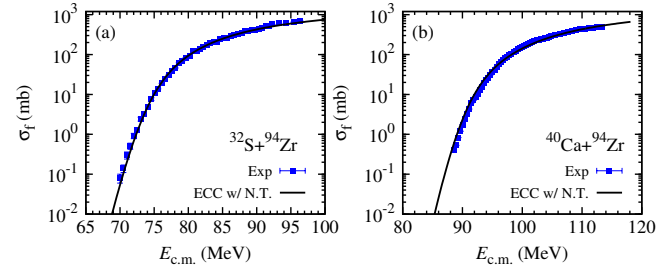


Figure 5 (Color online) The calculated and experimental fusion excitation functions for the reactions (a) $^{32}\text{S} + ^{94}\text{Zr}$ and (b) $^{40}\text{Ca} + ^{94}\text{Zr}$. The calculated fusion excitation functions are obtained from ECC calculations with the neutron transfer effects taken into account. The quadrupole deformation parameter $\beta_2 = 0.217$ for ^{94}Zr is used. The solid squares denote the experimental values taken from Refs. [39, 41].

Next let's discuss the discrepancies between the calculated fusion cross sections and the experimental values from another viewpoint: We first estimate the effect of coupling to the PQNT channels, then constrain the coupling effects due to inelastic excitation channels. Within the ECC model, for $^{32}\text{S} + ^{94,96}\text{Zr}$ and $^{40}\text{Ca} + ^{94,96}\text{Zr}$, the influence of neutron transfer should be almost the same because $Q(2n)$ values for these four reactions are very similar (see Table 1). As discussed in Sec. 3.1, the total effect of the couplings to the inelastic excitations and neutron transfer channels in $^{32}\text{S} + ^{94}\text{Zr}$ ($^{40}\text{Ca} + ^{94}\text{Zr}$) is also almost the same as that in $^{32}\text{S} + ^{96}\text{Zr}$ ($^{40}\text{Ca} + ^{96}\text{Zr}$). Therefore the enhancement of the fusion cross section due to couplings to inelastic excitations channels in reactions with ^{94}Zr and ^{96}Zr should be similar to each other. This implies that the structure information related to fusion as described by the ECC model for ^{94}Zr and ^{96}Zr should be similar, i.e., the quadrupole deformation parameters β_2 's for ^{94}Zr and ^{96}Zr should be similar to each other in ECC calculations. In order to check this conjecture, we calculate the fusion cross sections with $\beta_2 = 0.217$ for ^{94}Zr , the same as that of ^{96}Zr . The results obtained from ECC calculations with the PQNT effect taken into account are shown in Fig. 5. One can find that the calculated fusion cross sections are in good agreement with the data. In addition, as can be seen in Fig. 4(c) and Fig. 4(d), the relative enhancements of the reactions with ^{94}Zr as target are almost the same as those of the reactions with ^{96}Zr as target.

3.3 The issue of quadrupole deformation for ^{94}Zr

Within the ECC model [62], the formulas for calculating the parameters of the barrier distribution were proposed based on the quadrupole deformation parameters β_2 predicted by the FRDM [65]. According to the FRDM, $\beta_2 = 0.062$ for ^{94}Zr and $\beta_2 = 0.217$ for ^{96}Zr ; they are quite different.

As discussed before, the total effect of couplings to inelastic excitations and neutron transfer channels on fusion in the reaction $^{32}\text{S} + ^{94}\text{Zr}$ ($^{40}\text{Ca} + ^{94}\text{Zr}$) is almost the same as that in the reaction $^{32}\text{S} + ^{96}\text{Zr}$ ($^{40}\text{Ca} + ^{96}\text{Zr}$). On one hand, according to the estimate of the enhancement due to inelastic excitations channel couplings obtained from ECC calculations with $\beta_2 = 0.062$ for ^{94}Zr and $\beta_2 = 0.217$ for ^{96}Zr , one may conclude that the role of PQNT channels in the reactions with ^{94}Zr as target should be very different from that in the reactions with ^{96}Zr as target. On the other hand, within the ECC model, the role of PQNT channels in $^{32}\text{S} + ^{94,96}\text{Zr}$ and $^{40}\text{Ca} + ^{94,96}\text{Zr}$ should be similar because the $Q(2n)$ values are similar in these four reactions. This implies that the quadrupole deformation parameters of ^{94}Zr and ^{96}Zr should be similar to each other. Indeed, if one assumes that the quadrupole deformation parameter of ^{94}Zr is the same as that of ^{96}Zr , i.e., $\beta_2 = 0.217$, the fusion cross sections for reactions with ^{94}Zr as target from the ECC model are in good agreement with the experiment (see Fig. 5).

Therefore, it becomes a puzzling issue whether the quadrupole deformation parameters for ^{94}Zr and ^{96}Zr are similar to each other or not. In Table 3 we present β_2 values of ^{94}Zr and ^{96}Zr given in Refs. [73, 74]. The quadrupole deformation parameters deduced from $B(E2; \text{g.s.} \rightarrow 2_1^+)$ for ^{94}Zr and ^{96}Zr are quite small, but very close to each other, $\beta_2(^{94}\text{Zr}) = 0.09$ and $\beta_2(^{96}\text{Zr}) = 0.08$ [73]. In Ref. [74], a relativistic mean-field model was adopted to study the structural evolution in transition nuclei including ^{94}Zr and ^{96}Zr . With the NL3 interaction, the obtained β_2 's for ^{94}Zr and ^{96}Zr are 0.169 and 0.243, which are also similar. However, with the NL3* interaction, the obtained β_2 's for ^{94}Zr and ^{96}Zr are 0.002 and 0.233, which are quite different.

Table 3 The quadrupole deformation parameters for ^{94}Zr and ^{96}Zr .

β_2	FRDM [65]	RMF (NL3) [74]	RMF (NL3*) [74]	Expt. [73]
^{94}Zr	0.062	0.169	0.002	0.09
^{96}Zr	0.217	0.243	0.233	0.08

To solve this puzzling issue and get further understanding of the coupling to PQNT channels, we suggest to measure the fusion excitation function of the reactions $^{48}\text{Ca} + ^{94}\text{Zr}$ or $^{36}\text{S} + ^{94}\text{Zr}$. In these two reactions, the PQNT channels are closed (see Table 1). Therefore, these two reactions can be used to test the structure information connected to fusion of the target ^{94}Zr . If the results obtained from ECC calculations together with the quadrupole deformation parameters predicted from FRDM are in good agreement with the measured fusion excitation functions, one can conclude that the influence of PQNT channel coupling on sub-barrier fusion cross section

in the reaction $^{32}\text{S} + ^{94}\text{Zr}$ ($^{40}\text{Ca} + ^{94}\text{Zr}$) is stronger than that in the reaction $^{32}\text{S} + ^{96}\text{Zr}$ ($^{40}\text{Ca} + ^{96}\text{Zr}$). Otherwise, further study of the structure related to fusion of ^{94}Zr are needed. In any case, we can get a better understanding of the coupling to PQNT channels.

4 Summary

In summary, we adopt the universal fusion function formalism and the ECC model to investigate the dynamic coupling effects on fusion cross sections for the reactions $^{32}\text{S} + ^{94,96}\text{Zr}$ and $^{40}\text{Ca} + ^{94,96}\text{Zr}$. The reduced fusion excitation functions show that the total effect of inelastic excitations and neutron transfer channel couplings on fusion in $^{32}\text{S} + ^{94}\text{Zr}$ ($^{40}\text{Ca} + ^{94}\text{Zr}$) is almost the same as that in $^{32}\text{S} + ^{96}\text{Zr}$ ($^{40}\text{Ca} + ^{96}\text{Zr}$). Within the ECC model, the enhancements due to inelastic excitations channel couplings and neutron transfer channel coupling are evaluated separately. The results show that influences of neutron transfer in the reactions with ^{94}Zr as target should be almost the same as that in the reactions with ^{96}Zr as target. This implies that the quadrupole deformation parameters of ^{94}Zr and ^{96}Zr should be similar to each other. However, the quadrupole deformation parameters predicted from FRDM used in the ECC model are quite different. Experiments on $^{48}\text{Ca} + ^{94}\text{Zr}$ or $^{36}\text{S} + ^{94}\text{Zr}$ are suggested to solve the puzzling issue of whether the quadrupole deformation parameters for ^{94}Zr and ^{96}Zr are similar to each other or not.

This work has been partly supported by the National Key Basic Research Program of China (Grant No. 2013CB834400), the National Natural Science Foundation of China (Grants No. 11175252, No. 11120101005, No. 11275248, No. 11475115, and No. 11525524), and the Knowledge Innovation Project of the Chinese Academy of Sciences (Grant No. KJCX2-EW-N01). The computational results presented in this work have been obtained on the High-performance Computing Cluster of SKLTP/ITP-CAS and the Sc-Grid of the Supercomputing Center, Computer Network Information Center of the Chinese Academy of Sciences.

- Balantekin A B, Takigawa N. Quantum tunneling in nuclear fusion. *Rev Mod Phys*, 1998, 70: 77–100
- Dasgupta M, Hinde D J, Rowley N, et al. Measuring barriers to fusion. *Annu Rev Nucl Part Sci*, 1998, 48: 401–461
- Canto L F, Gomes P R S, Donangelo R, et al. Fusion and breakup of weakly bound nuclei. *Phys Rep*, 2006, 424: 1–111
- Back B B, Esbensen H, Jiang C L, et al. Recent developments in heavy-ion fusion reactions. *Rev Mod Phys*, 2014, 86: 317–360
- Meißner U G. Anthropoc considerations in nuclear physics. *Science Bulletin*, 2014, 60: 43–54
- Canto L F, Gomes P R S, Donangelo R, et al. Recent developments in fusion and direct reactions with weakly bound nuclei. *Phys Rep*, 2015, 596: 1–86
- Fu C, Bao J, Chen L, et al. Laser-driven plasma collider for nuclear studies. *Science Bulletin*, 2015, 60: 1211–1213
- Adamian G G, Antonenko N V, Scheid W. Model of competition between fusion and quasifission in reactions with heavy nuclei. *Nucl Phys A*, 1997, 618: 176–198

- 9 Adamian G G, Antonenko N V, Scheid W, et al. Fusion cross sections for superheavy nuclei in the dinuclear system concept. *Nucl Phys A*, 1998, 633: 409–420
- 10 Adamian G G, Antonenko N V, Tchuvil'sky Y M. Effect of structural forbiddenness in fusion of heavy nuclei. *Phys Lett B*, 1999, 451: 289–295
- 11 Knyazheva G N, Kozulin E M, Sagaidak R N, et al. Quasifission processes in $^{40,48}\text{Ca}+^{144,154}\text{Sm}$ reactions. *Phys Rev C*, 2007, 75: 064602–13
- 12 Wang N, Zhao E G, Scheid W, et al. Theoretical study of the synthesis of superheavy nuclei with $Z = 119$ and 120 in heavy-ion reactions with trans-uranium targets. *Phys Rev C*, 2012, 85: 041601(R)–5
- 13 Wang N, Zhao E, Zhou S G. Study of nuclear dynamical deformation in the synthesis of super-heavy nuclei. *J Phys: Conf Ser*, 2014, 515: 012022–8
- 14 Zhang J, Wang C, Ren Z. Calculation of evaporation residue cross sections for the synthesis of superheavy nuclei in hot fusion reactions. *Nucl Phys A*, 2013, 909: 36–49
- 15 Shen J J, Shen C W. Theoretical analysis of mass distribution of quasifission for ^{238}U -induced reactions. *Sci China-Phys Mech Astron*, 2014, 57: 454–457
- 16 Fan X, Dong J, Zuo W. Symmetry energy at subsaturation densities and the neutron skin thickness of ^{208}Pb . *Science China Physics, Mechanics & Astronomy*, 2015, 58: 062002–5
- 17 Mo Q, Liu M, Cheng L, et al. Deformation dependence of symmetry energy coefficients of nuclei. *Sci China-Phys Mech Astron*, 2015, 58: 082001–6
- 18 Jiang C L, Esbensen H, Rehm K E, et al. Unexpected Behavior of Heavy-Ion Fusion Cross Sections at Extreme Sub-Barrier Energies. *Phys Rev Lett*, 2002, 89: 052701–4
- 19 Misicu S, Esbensen H. Hindrance of Heavy-Ion Fusion due to Nuclear Incompressibility. *Phys Rev Lett*, 2006, 96: 112701–4
- 20 Dasgupta M, Hinde D J, Diaz-Torres A, et al. Beyond the Coherent Coupled Channels Description of Nuclear Fusion. *Phys Rev Lett*, 2007, 99: 192701–4
- 21 Diaz-Torres A, Hinde D, Dasgupta M, et al. Dissipative quantum dynamics in low-energy collisions of complex nuclei. *Phys Rev C*, 2008, 78: 064604–6
- 22 Ichikawa T, Hagino K, Iwamoto A. Signature of Smooth Transition from Sudden to Adiabatic States in Heavy-Ion Fusion Reactions at Deep Sub-Barrier Energies. *Phys Rev Lett*, 2009, 103: 202701–4
- 23 Denisov V Y. Nucleus-nucleus potential with shell-correction contribution and deep sub-barrier fusion of heavy nuclei. *Phys Rev C*, 2014, 89: 044604–6
- 24 Gomes P R S, Linares R, Lubian J, et al. Search for systematic behavior of incomplete-fusion probability and complete-fusion suppression induced by ^9Be on different targets. *Phys Rev C*, 2011, 84: 014615–7
- 25 Sargsyan V V, Adamian G G, Antonenko N V, et al. Search for a systematic behavior of the breakup probability in reactions with weakly bound projectiles at energies around the Coulomb barrier. *Phys Rev C*, 2012, 86: 054610–9
- 26 Gasques L R, Hinde D J, Dasgupta M, et al. Suppression of complete fusion due to breakup in the reactions $^{10,11}\text{B}+^{209}\text{Bi}$. *Phys Rev C*, 2009, 79: 034605–8
- 27 Dasgupta M, Gasques L R, Luong D H, et al. Reaction dynamics of weakly bound nuclei at near-barrier energies. *Nucl Phys A*, 2010, 834: 147c–150c
- 28 Beckerman M, Salomaa M, Sperduto A, et al. Dynamic Influence of Valence Neutrons upon the Complete Fusion of Massive Nuclei. *Phys Rev Lett*, 1980, 45: 1472–1475
- 29 Broglia R, Dasso C, Landowne S, et al. Possible effect of transfer reactions on heavy ion fusion at sub-barrier energies. *Phys Rev C*, 1983, 27: 2433–2435(R)
- 30 Broglia R A, Dasso C H, Landowne S, et al. Estimate of enhancements in sub-barrier heavy-ion fusion cross sections due to coupling to inelastic and transfer reaction channels. *Phys Lett B*, 1983, 133: 34–38
- 31 Stelson P H, Kim H J, Beckerman M, et al. Fusion cross sections for $^{46,50}\text{Ti}+^{90}\text{Zr}, ^{93}\text{Nb}$ and some systematics of heavy-ion fusion at barrier and subbarrier energies. *Phys Rev C*, 1990, 41: 1584–1599
- 32 Dasso C H, Landowne S, Winther A. Channel-coupling effects in heavy-ion fusion reactions. *Nucl Phys A*, 1983, 405: 381–396
- 33 Dasso C H, Landowne S, Winther A. A study of Q -value effects on barrier penetration. *Nucl Phys A*, 1983, 407: 221–232
- 34 Zhang G L, Liu X X, Lin C J. Systematic analysis of the effect of a positive Q -value neutron transfer in fusion reactions. *Phys Rev C*, 2014, 89: 054602–8
- 35 Wang B, Zhao W J, Gomes P R S, et al. Systematic study of breakup effects on complete fusion at energies above the Coulomb barrier. *Phys Rev C*, 2014, 90: 034612–9
- 36 Pengo R, Evers D, Löbner K, et al. Nuclear structure effects in sub-barrier fusion cross sections. *Nucl Phys A*, 1983, 411: 255–274
- 37 Aljuwair H, Ledoux R, Beckerman M, et al. Isotopic effects in the fusion of ^{40}Ca with $^{40,44,48}\text{Ca}$. *Phys Rev C*, 1984, 30: 1223–1227
- 38 Timmers H, Ackermann D, Beghini S, et al. A case study of collectivity, transfer and fusion enhancement. *Nucl Phys A*, 1998, 633: 421–445
- 39 Stefanini A, Behera B, Beghini S, et al. Sub-barrier fusion of $^{40}\text{Ca}+^{94}\text{Zr}$: Interplay of phonon and transfer couplings. *Phys Rev C*, 2007, 76: 014610–5
- 40 Zhang H Q, Lin C J, Yang F, et al. Near-barrier fusion of $^{32}\text{S}+^{90,96}\text{Zr}$: The effect of multi-neutron transfers in sub-barrier fusion reactions. *Phys Rev C*, 2010, 82: 054609–7
- 41 Jia H M, Lin C J, Yang F, et al. Fusion of $^{32}\text{S}+^{94}\text{Zr}$: Further exploration of the effect of the positive Q_{nn} value neutron transfer channels. *Phys Rev C*, 2014, 89: 064605
- 42 Jacobs P, Fraenkel Z, Mamane G, et al. Sub-coulomb barrier fusion of $\text{O}+\text{Sn}$. *Phys Lett B*, 1986, 175: 271–274
- 43 Jia H M, Lin C J, Yang F, et al. Fusion of the $^{16}\text{O}+^{76}\text{Ge}$ and $^{18}\text{O}+^{74}\text{Ge}$ systems and the role of positive Q -value neutron transfers. *Phys Rev C*, 2012, 86: 044621–6
- 44 Zagrebaev V I. Sub-barrier fusion enhancement due to neutron transfer. *Phys Rev C*, 2003, 67: 061601(R)–5
- 45 Sargsyan V V, Adamian G G, Antonenko N V, et al. Influence of neutron transfer in reactions with weakly and strongly bound nuclei on the sub-barrier capture process. *Phys Rev C*, 2012, 86: 014602–10
- 46 Sargsyan V V, Scamps G, Adamian G G, et al. Neutron-pair transfer in the sub-barrier capture process. *Phys Rev C*, 2013, 88: 064601–7
- 47 Sargsyan V V, Adamian G G, Antonenko N V, et al. Examination of the different roles of neutron transfer in the sub-barrier fusion reactions $^{32}\text{S}+^{94,96}\text{Zr}$ and $^{40}\text{Ca}+^{94,96}\text{Zr}$. *Phys Rev C*, 2015, 91: 014613–7
- 48 Hagino K, Rowley N, Kruppa A T. A program for coupled-channel calculations with all order couplings for heavy-ion fusion reactions. *Comput Phys Commun*, 1999, 123: 143–152
- 49 Wang N, Li Z, Wu X. Improved quantum molecular dynamics model and its applications to fusion reaction near barrier. *Phys Rev C*, 2002, 65: 064608–10
- 50 Wang N, Zhao K, Li Z. Systematic study of ^{16}O -induced fusion with the improved quantum molecular dynamics model. *Phys Rev C*, 2014, 90: 054610
- 51 Wang N, Li Z, Wu X, et al. Further development of the improved quantum molecular dynamics model and its application to fusion reactions near the barrier. *Phys Rev C*, 2004, 69: 034608–9
- 52 Wen K, Sakata F, Li Z X, et al. Non-Gaussian Fluctuations and Non-Markovian Effects in the Nuclear Fusion Process: Langevin Dynamics Emerging from Quantum Molecular Dynamics Simulations. *Phys Rev Lett*, 2013, 111: 012501–5

- 53 Wen K, Sakata F, Li Z X, et al. Energy dependence of the nucleus-nucleus potential and the friction parameter in fusion reactions. *Phys Rev C*, 2014, 90: 054613–12
- 54 Wang N, Zhao K, Li Z. Fusion and quasi-fission dynamics in nearly-symmetric reactions. *Science China Physics, Mechanics & Astronomy*, 2015, 58: 112001
- 55 Umar A S, Oberacker V E. Heavy-ion interaction potential deduced from density-constrained time-dependent Hartree-Fock calculation. *Phys Rev C*, 2006, 74: 021601(R)–3
- 56 Umar A S, Oberacker V E, Maruhn J A, et al. Microscopic composition of ion-ion interaction potentials. *Phys Rev C*, 2012, 85: 017602–5
- 57 Keser R, Umar A S, Oberacker V E. Microscopic study of Ca + Ca fusion. *Phys Rev C*, 2012, 85: 044606–10
- 58 Guo L, Maruhn J A, Reinhard P G. Boost-invariant mean field approximation and the nuclear Landau-Zener effect. *Phys Rev C*, 2007, 76: 014601–7
- 59 Guo L, Maruhn J A, Reinhard P G, et al. Conservation properties in the time-dependent Hartree Fock theory. *Phys Rev C*, 2008, 77: 041301(R)–4
- 60 Dai G F, Guo L, Zhao E G, et al. Effect of tensor force on dissipation dynamics in time-dependent Hartree-Fock theory. *Sci China-Phys Mech Astron*, 2014, 57: 1618–1622
- 61 Dai G F, Guo L, Zhao E G, et al. Dissipation dynamics and spin-orbit force in time-dependent Hartree-Fock theory. *Phys Rev C*, 2014, 90: 044609–7
- 62 Wang B, Wen K, Zhao W J, et al. Systematics of capture and fusion dynamics in heavy-ion collisions. *arXiv:1504.00756 [nucl-th]*, 2015
- 63 Hill D L, Wheeler J A. Nuclear Constitution and the Interpretation of Fission Phenomena. *Phys Rev*, 1953, 89: 1102–1145
- 64 Li L L, Zhou S G, Zhao E G, et al. A new barrier penetration formula and its application to alpha-decay half-lives. *Int J Mod Phys E*, 2010, 19: 359–370
- 65 Möller P, Nix J R, Myers W D, et al. Nuclear Ground-State Masses and Deformations. *At Data Nucl Data Tables*, 1995, 59: 185–381
- 66 Canto L F, Gomes P R S, Lubian J, et al. Disentangling static and dynamic effects of low breakup threshold in fusion reactions. *J Phys G: Nucl Part Phys*, 2009, 36: 015109–9
- 67 Canto L F, Gomes P R S, Lubian J, et al. Dynamic effects of breakup on fusion reactions of weakly bound nuclei. *Nucl Phys A*, 2009, 821: 51–71
- 68 Stefanini A, Scarlassara F, Beghini S, et al. Fusion of $^{48}\text{Ca} + ^{90,96}\text{Zr}$ above and below the Coulomb barrier. *Phys Rev C*, 2006, 73: 034606
- 69 Cândido Ribeiro M A, Chamon L C, Pereira D, et al. Pauli Nonlocality in Heavy-Ion Rainbow Scattering: A Further Test of the Folding Model. *Phys Rev Lett*, 1997, 78: 3270–3273
- 70 Chamon L C, Pereira D, Hussein M S, et al. Nonlocal Description of the Nucleus-Nucleus Interaction. *Phys Rev Lett*, 1997, 79: 5218–5221
- 71 Chamon L C, Carlson B V, Gasques L R, et al. Toward a global description of the nucleus-nucleus interaction. *Phys Rev C*, 2002, 66: 014610–13
- 72 Wong C Y. Interaction Barrier in Charged-Particle Nuclear Reactions. *Phys Rev Lett*, 1973, 31: 766–769
- 73 Raman S, Nestor C W, Tikkanen P. Transition probability from the ground to the first-excited 2^+ state of even-even nuclides. *At Data Nucl Data Tables*, 2001, 78: 1–128
- 74 Bhuyan M. Structural evolution in transitional nuclei of mass $82 \leq A \leq 132$. *Phys Rev C*, 2015, 92: 034323–10